Ceramics-Silikáty 63 (2), 232-238 (2019)
www.ceramics-silikaty.cz doi: 10.13168/cs.2019.0015

EFFECTS OF NH_4HCO_3 CONTENTS ON THE PROPERTIES OF SiC POROUS CERAMICS REINFORCED WITH WHISKERS

YINGYING ZHAI*, **, #BEIYUE MA**, YARAN ZHANG**, #XINMING REN**, HUA WU**, FAN QIAN***, WENGANG YANG***, GUOQI LIU***, QIANG ZHU****

*Computing Center, Northeastern University, Shenyang 110819, P.R. China
**School of Metallurgy, Northeastern University, Shenyang 110819, P.R. China
***State Key Lab for Advanced Refractories, Sinosteel Luoyang Institute of Refractories Research Co., Ltd., Luoyang 471039, P.R. China
****Electron Microscope Unit, Mark Wainwright Analytical Centre, The University of New South Wales, Sydney, NSW 2032, Australia

#E-mail: maby@smm.neu.edu.cn, renxm1124@163.com

Submitted January 30, 2019; accepted March 18, 2019

Keywords: SiC porous ceramics, Pore-forming, Whisker, Crystalline silicon cutting slurry waste

SiC porous ceramics (SPCs) were prepared from crystalline silicon cutting slurry waste with NH_4HCO_3 (NHC) as the pore-forming agent. The effects of NHC contents on the properties of the as-prepared SPCs were investigated. It was found that the main crystalline phase of the SPCs was β-SiC. The SPCs consisted of SiC particles and SiC whiskers. The thermal shock resistance of the SPCs was obviously strengthened due to the formation of the SiC whisker. When NHC contents were increased to 30 wt. %, the cold compressive strength and thermal shock resistance of the SPCs with porosity of around 63.76 % were found to be favourable to the application in the molten metal filtration field.

INTRODUCTION

Crystalline silicon cutting slurry waste exists in the form of slurry mixed with cutting fluid, Si particles, abrasive SiC particles and metals worn down from a saw wire, which is an industrial by-product in the process of multi-crystalline silicon cutting. More than 50 % of Si becomes powder and goes into the slurry waste in the process of wafer slicing [1]. Moreover, the amount of crystalline silicon waste, released by the global photovoltaic industry, has been increasing throughout the world [2-3]. Therefore, an environment-friendly and sustainable development method is critically required to recycle the crystalline silicon waste. However, the process of separating SiC and Si is difficult due to the similar physical and chemical properties [4].

SiC porous ceramics (SPCs) have drawn strong attention due to their excellent physical and chemical properties, including high mechanical strength, high temperature resistance, excellent oxidation resistance and corrosion resistance. They have been widely applied in catalyst carriers and heat exchangers or heat insulation [5-7]. As for now, some proven technologies have been used to prepare SPCs; for instance, the pore-forming method, sacrificial template method, freeze-casting method, gel-casting method, chemical vapour infiltration and 3-D printing [8-10]. However, it is worth noting that SPCs generally have a shortage of low strength and instability. Although whisker toughening is currently an effective solution, the complex process and expensive costs limit its further development and large-scale application [11-13].

In the present work, SPCs reinforced with in-situ formed SiC whisker were successfully fabricated by adding the pore forming agent method using crystalline silicon cutting slurry waste. This method is convenient, low-cost and environment-friendly, which makes it become a promising way for recycling solid waste. Additionally, the effects of NHC contents on the properties of the as-prepared SPCs have been studied. To our knowledge, this is the first report on the preparation of in-situ SiC whisker reinforced SiC porous ceramics using crystalline silicon cutting slurry waste as the main raw material.

EXPERIMENTAL

Raw materials

The crystalline silicon cutting slurry waste (average size of 74 μm) with the following chemical compositions: 69.00 wt. % SiC, 11.93 wt. % Si, 8.28 wt. % SiO_2, 7.50 wt. % Fe_2O_3 and 3.29 wt. % LOI was used. Activated carbon (analytical grade purity, Sinopharm

Chemical Reagent Co., Ltd., China) was taken as the source of carbon. Phenolic resin (Industrial-grade purity reagent) was chosen as the binder. NHC (analytical grade purity, Sinopharm Chemical Reagent Co., Ltd., China) was used as the pore-forming agent. In addition, the volume fraction of the argon gas was 99.99 %.

Preparation processes

During the preparation process of the SPCs, Si and SiO_2 in the crystalline silicon waste reacted with carbon to form SiC, and the chemical reactions can be represented by:

$$\text{Si (l)} + \text{C (s)} \rightarrow \text{SiC (s)} \quad (1)$$

$$\text{SiO}_2\text{ (s)} + 3\text{C (s)} \rightarrow \text{SiC (s)} + 2\text{CO (g)} \quad (2)$$

According to reactions 1 and 2, the mass ratio of the crystalline silicon waste to the activated carbon was calculated and determined as 100:15. Additionally, the raw materials were mixed with 5 wt. % Phenolic resin. The samples doped with various amounts of NHC, which were 0, 10, 20, 30 wt. %, and the corresponding samples were identified as N0-N3.

The fabrication process of the SPCs used the following procedures: Firstly, the crystalline silicon waste, activated carbon, phenolic resin and NHC were weighed and homogeneously milled using an agate mortar for 30 min. Secondly, the mixed ceramic raw materials were pressed to form the samples under 100 MPa for 5 min, and the sample size was 15 mm in diameter and 10 ~ 15 mm in thickness. Finally, all the green bodies were sintered in argon with the proper temperature-programmed to 1500 °C for 4 h. A detailed description of the fabrication process can be found in Ref. [14].

Characterisation

The microstructures were observed by scanning electron microscope (SEM, ZEISS-EVO18, Germany) equipped with a dispersive energy spectrum (EDS). The phase compositions were characterised via X-ray diffraction (XRD, Cu Kα radiation, 30 kV and 30 mA). The apparent porosity and bulk density of the sintered samples were measured according to Archimedes law and they were calculated based on Equations 3 and 4.

$$P_a = \frac{m_3 - m_1}{m_3 - m_2} \times 100\ \% \quad (3)$$

$$D_b = \frac{m_1\, d}{m_3 - m_2} \quad (4)$$

where P_a and D_b are the apparent porosity (%) and bulk density (g·cm^{-3}) of the tested sample, m_1 is the mass of the dried sample in air (g), m_2 is the mass of the sample in water (g), m_3 is the mass of the sample with free bubbles on the surface (g), and d is the density of water (1.0 g·cm^{-3}).

In addition, the pore size distribution of the as-sintered samples was measured by mercury intrusion porosimetry (MIP) and according to Equation 5.

$$r = -\left(\frac{2\sigma \cos\theta}{P}\right) \quad (5)$$

where r is the pore size of the tested sample, P is the pressure applied during the test, σ is the surface tension of mercury, and θ is the contact angle of mercury and the tested sample.

The Chinese standards of GB/T 1964-1996 were followed for the compressive strength test. The thermal shock resistance is characterised by the number of thermal cycles. The specific operation method is as follows: the samples were transferred into an electric furnace at 1000 °C and held for 15 min, and then quenched in air for 10 min, and returning them to the furnace at 1000 °C again. It is noted that the samples completed 100 cycles between 1000 °C and room temperature in air, the quenched medium was changed to water. The total thermal cycling numbers to the cracking were used to characterise the thermal shock resistance of the SPCs [15].

RESULTS AND DISCUSSION

XRD and SEM analyses

The XRD patterns of the as-prepared SPCs are shown in Figure 1. It can be observed that 3C-SiC (cubic crystal), 6H-SiC (hexagonal crystal), small amounts of FeSi and remnant SiO_2 peaks can be detected in the final products, which means that SiO_2 in the raw material

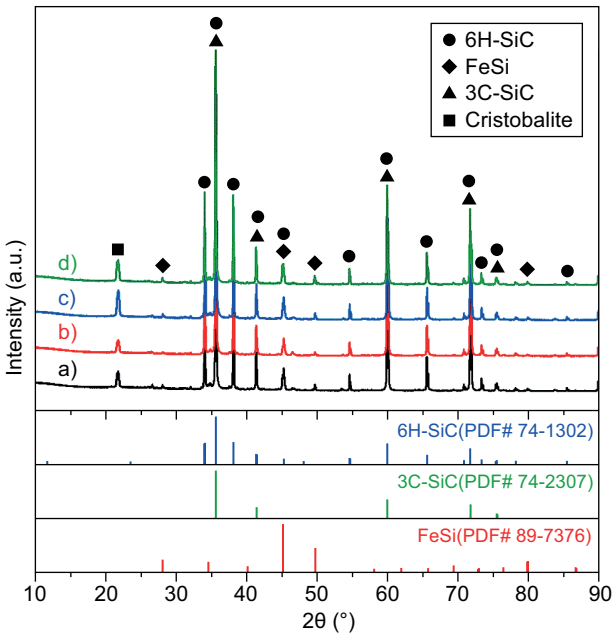

Figure 1. The XRD patterns of the as-prepared SPCs doped with different amounts of NHC: a-d) are samples N0-N3, respectively.

did not fully react with C. Fe_2O_3 was converted to FeSi. In addition, with the increase of NHC contents, the diffraction intensities of the above phases are almost constants (Figure 1a-d), which indicates that the addition of NHC has hardly any effect on the constituents of the as-prepared SPCs.

The SEM images in Figure 2 show the SPCs mainly consist of particles and whiskers. The particles were irregular or polygonal in shape, a small part of the whiskers are inserted in the holes of the SiC matrix, and the rest covered the surface of the particles. The corresponding EDS analysis indicates that the whiskers

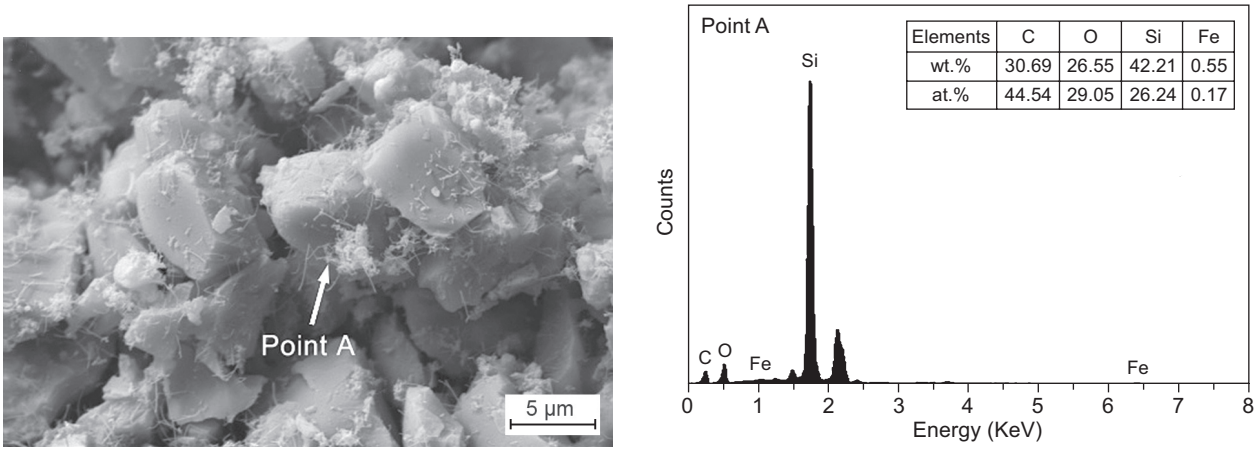

a) N0

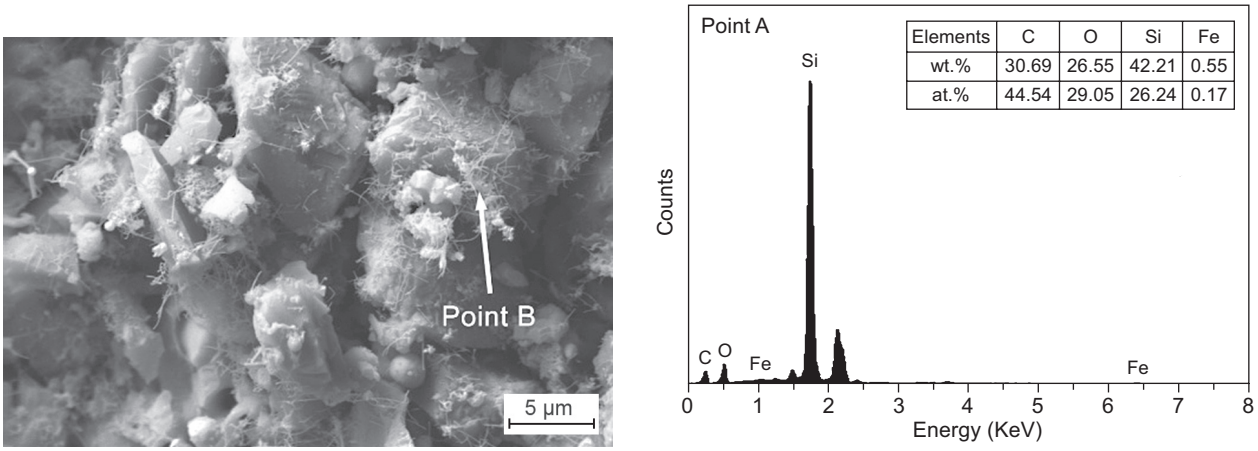

b) N1

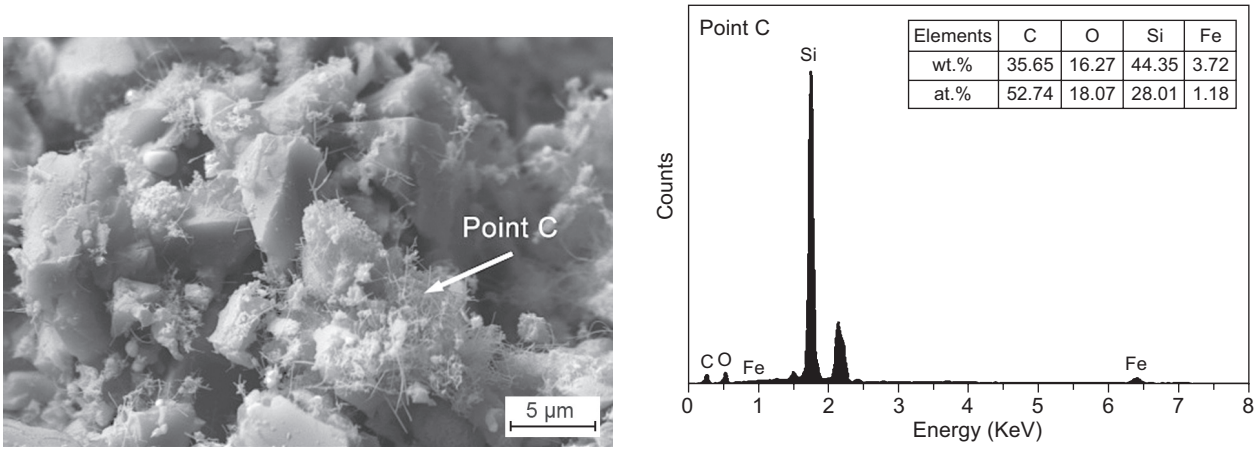

c) N2

Figure 2. The cross-section SEM images and EDS spectra of the as-prepared SPCs doped with different amounts of NHC: a-d) are samples N0-N3, respectively. *(Continue on next page)*

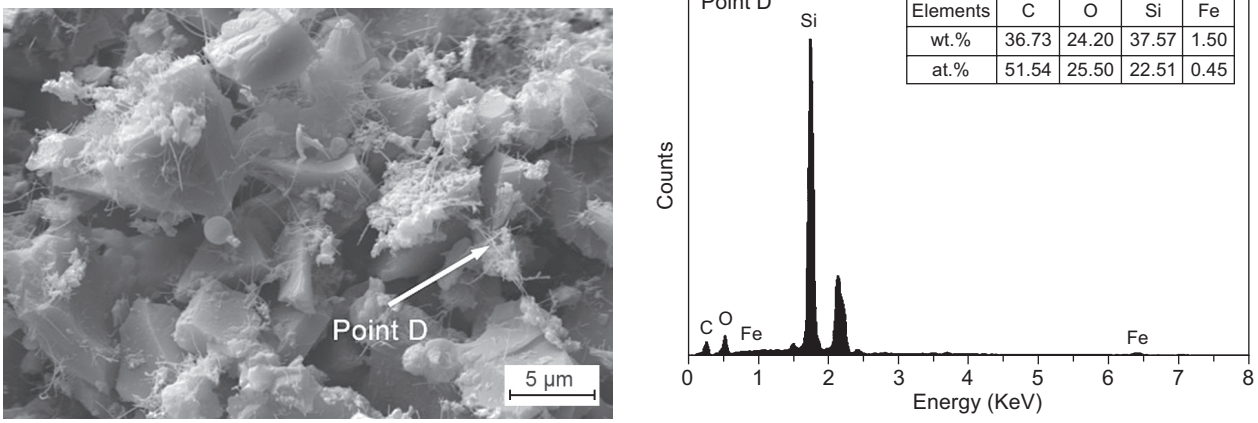

d) N3

Figure 2. The cross-section SEM images and EDS spectra of the as-prepared SPCs doped with different amounts of NHC: a-d) are samples N0-N3, respectively.

are mainly composed of Si, C, O elements and a small amount of Fe element. The finding is consistent with the above analysis results of the XRD patterns.

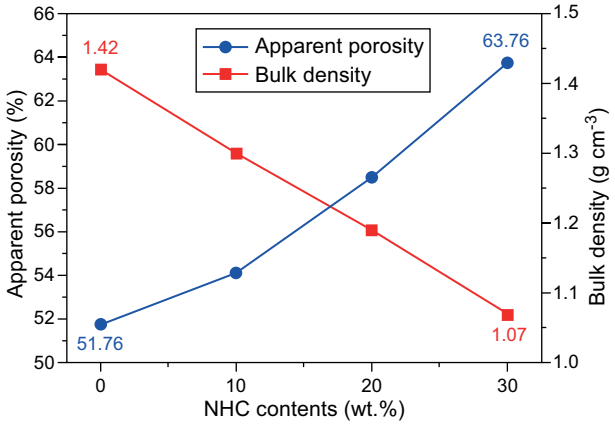

a)

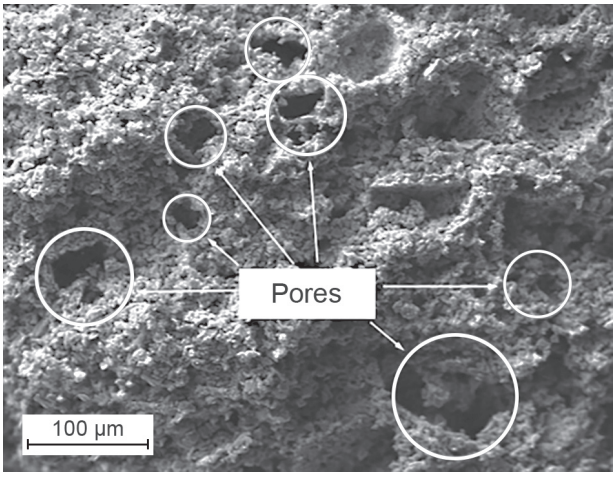

b)

Figure 3. The apparent porosity and bulk density of the SPCs doped with different amounts of NHC (a) and the SEM image of sample N3 sintered at 1500 °C for 4 h (b).

Sintering character

As shown in Figure 3a, the apparent porosity of the SPCs is increased when increasing the addition amount of NHC, while the bulk density is decreased. This ascribes to the decomposition of NHC and original pores in the green compacts [16]. When the addition amount of NHC is 30 wt. %, the SPCs can reach the maximum apparent porosity, which is 63.76 %. At the same time, the bulk density of it is the minimum, 1.07 g·cm^{-3}. This can be visualised in the micrograph of sample N3 (Figure 3b). The surface of the sample is evenly distributed with pores formed by pyrolysis of the pore former.

Figure 4 compares the pore size distribution of the SPCs doped with different amounts of NHC. It can be clearly seen that the aperture range of the SPCs is around 1 μm. The amount of the pore former (NHC) added has rarely an effect on the pore size distribution. Generally, the pore size is related to the compact degree

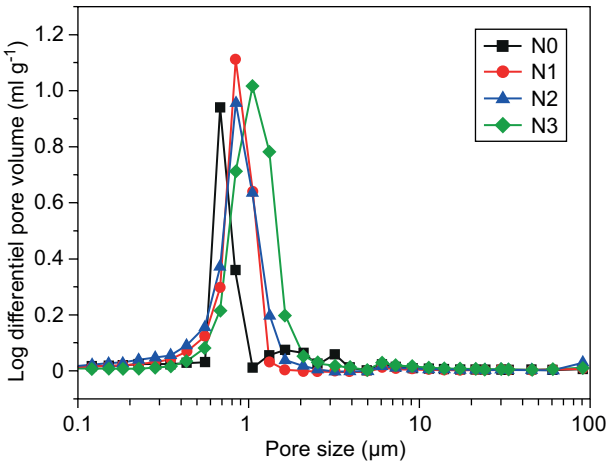

Figure 4. The pore size distribution of the SPCs doped with different amounts of NHC.

of the sintering. That is, a higher sintering temperature or a larger addition of sintering-aids results in a smaller median pore diameter [12, 14]. Since the SPCs doped with different amounts of NHC were prepared at the same sintering temperature, and the pore former did not affect the pore size distribution, the pore size distribution tendency of the samples is almost the same as shown.

Cold compressive strength and thermal shock resistance

As shown in Figure 5, the compressive strength shows a decreasing trend, which can be attributed to the increase of the apparent porosity due to the increase of NHC. It is known that cracks are usually found before 50 thermal shock cycles cooled in air [17], but the number of thermal cycles of the SPCs reinforced with SiC whiskers is more than 100 times. Hence, it can be concluded that the SiC whiskers are possibly beneficial in enhancing the thermal shock resistance of the SPCs. The sample with excellent thermal shock resistance favours its application in the molten metal filtration field [15].

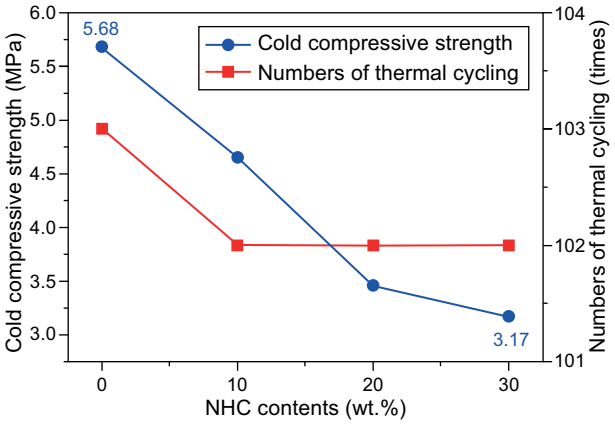

Figure 5. The cold compressive strength and thermal shock resistance of the SPCs doped with different amounts of NHC (N0-N3).

Analysis of the whisker formation process

Generally, SiC whiskers can be formed by two mechanisms: the vapour-solid theory (VS) and the vapour-liquid-solid theory (VLS). Due to the catalytic action of metals such as Fe, Co and Ni, the formation temperature of SiC whiskers is lower in the VLS system [18-20]. In this paper, Fe and FeSi (melting point: 1410 °C) act as the catalysis in the preparation of SiC whiskers. Iron is formed via the reaction 3 of Fe_2O_3 and C in the raw materials, and then a part of the Fe reacts with Si to form FeSi (reaction 7).

$$C\,(s) + Fe_2O_3\,(s) \rightarrow Fe\,(s) + CO \quad (6)$$

$$Si\,(s) + Fe\,(s) \rightarrow FeSi\,(s) \quad (7)$$

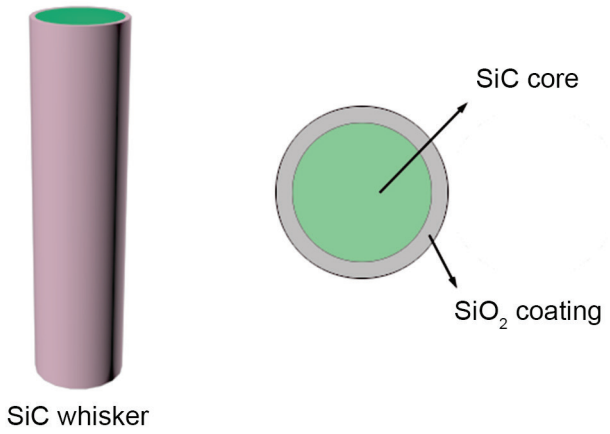

Figure 6. The sketch of the double-layered whisker formed by using SiO_2 as the starting nucleus.

As the temperature rises, Fe and FeSi gradually melt and enclose the surrounding C particles and SiO_2 particles. Meanwhile, some further reactions (reactions (8)-(15)) produce several gas phases which are necessary for the formation of the SiC whiskers. Studies have shown that SiO_2 can be used as the starting nucleus for the formation of the SiC whiskers [21]. Whiskers formed in this way are of a two-layer structure. A schematic diagram of this double-layer is shown in Figure 6.

$$Si\,(s) \rightarrow Si\,(l) \quad (8)$$

$$\Delta G_8^{\theta}\,(J{\cdot}mol^{-1}) = 50\,540 - 30.0\,T\,(K) \quad (9)$$

$$Si\,(l) \rightarrow Si\,(g) \quad (10)$$

$$\Delta G_8^{\theta}\,(J{\cdot}mol^{-1}) = 395\,400 - 111.38\,T\,(K) \quad (11)$$

$$Si\,(l) + SiO_2\,(s) \rightarrow 2SiO\,(g) \quad (12)$$

$$\Delta G_8^{\theta}\,(J{\cdot}mol^{-1}) = 635\,890 - 292.2\,T\,(K) \quad (13)$$

$$C\,(s) + SiO_2\,(s) \rightarrow SiO\,(g) + CO\,(g) \quad (14)$$

$$\Delta G_8^{\theta}\,(J{\cdot}mol^{-1}) = 676\,720 - 330.69\,T\,(K) \quad (15)$$

As shown in the reactions below, these gas phase products are dissolved in Fe and FeSi droplets and react with the corresponding solid particles (C or SiO_2) to form β-SiC crystals. When the SiC crystals reach saturation in the droplets, they begin to precipitate out and continue to grow along a definitive crystal orientation.

$$2\,C\,(s) + SiO\,(g) \rightarrow SiC\,(s) + CO\,(g) \quad (16)$$

$$\Delta G_8^{\theta}\,(J{\cdot}mol^{-1}) = -73\,570 - 1.29\,T\,(K) \quad (17)$$

At this point, the SiC whiskers are completely formed. Figure 7 visualises the entire preparation process. Combined with above analysis, it can be inferred that the SiC whiskers formation mechanism of this paper is the VLS system.

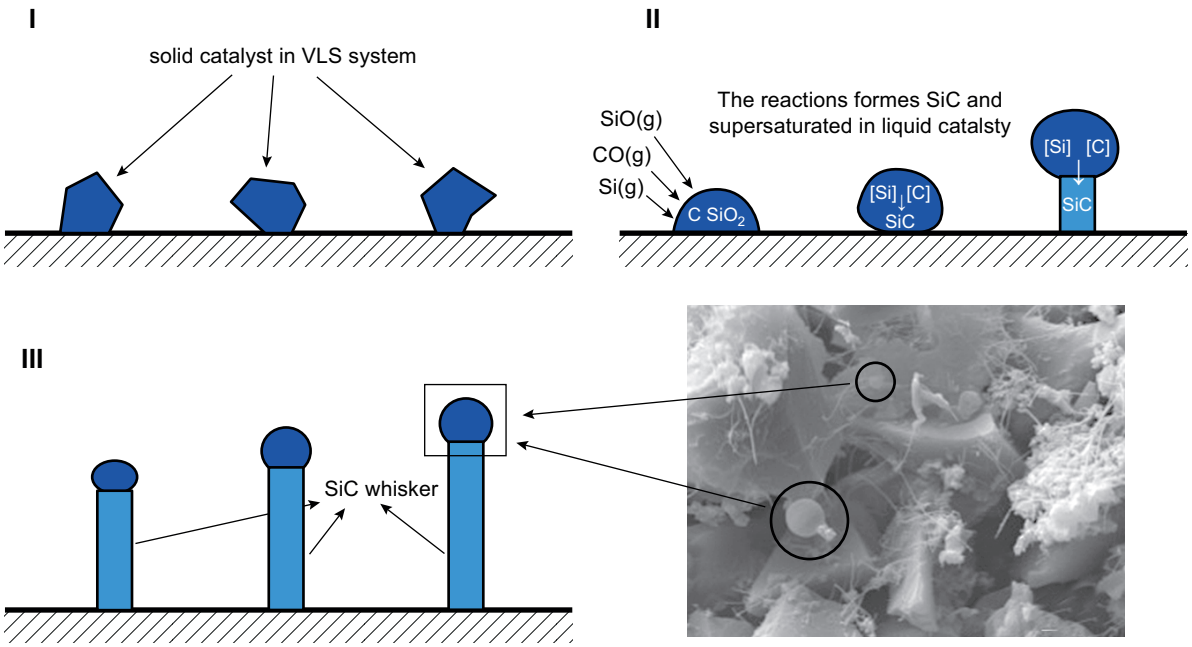

Figure 7. The schematic diagram of the SiC whiskers formation by the VLS mechanism.

CONCLUSIONS

The SiC porous ceramics prepared from crystalline silicon cutting slurry waste doped with 30 wt. % NHC displayed excellent properties, such as a high apparent porosity (63.76 %), high cold compressive strength (3.17 MPa), ultrahigh thermal shock resistance (thermal cycles number 102 times). During the preparation process of the SPCs, SiC whiskers were formed, and they are the good reinforcement phase for the fabrication of the SPCs.

Acknowledgments

The authors gratefully acknowledge the financial support from the open research fund for the State Key Lab for Advanced Refractories (SKLAR201904), Fundamental Research Fund for the Central Universities (Grant No. N171603015), and the National Natural Science Foundation of China (Grant No. 51772277).

REFERENCES

1. Li D.G., Xing P.F., Zhuang Y.X., Li F., Tu G.F. (2014): Recovery of high purity silicon from SoG crystalline silicon cutting slurry waste. Transactions of Nonferrous Metals Society of China, 24(4), 1237-1241. Doi: 10.1016/S1003-6326(14)63184-8
2. Zhao M., Johnson M., He W.Z., Li G.M., Zhao C., Huang J.W., Zhu H.C. (2017): Transformation of waste crystalline silicon into submicro β-SiC by multimode microwave sintering with low carbon emissions. Powder Technology, 332, 290-295. Doi: 10.1016/j.powtec.2017.09.024
3. Wang Y.X., Jiang C., Liang H.Y. (2012): Recovery and separation of Si and SiC in wire cutting waste slurry from photovoltaic silicon. Key Engineering Materials, 512-515, 1541-1544. Doi: 10.4028/www.scientific.net/KEM.512-515.1541
4. Hsu H.P., Huang W.P., Yang C.F., Lang C.W. (2014): Silicon recovery from cutting slurry by phase transfer separation. Separation and Purification Technology, 133, 1-7. Doi: 10.1016/j.seppur.2014.06.037
5. Ma B.Y., Ren X.M., Yin Y., Yuan L., Zhang Z., Li Z.Q., Li G.Q., Zhu Q., Yu J.K. (2017): Effects of processing parameters and rare earths additions on preparation of Al_2O_3-SiC composite powders from coal ash. Ceramics International, 43(15), 11830-11837. Doi: 10.1016/j.ceramint.2017.05.362
6. Yamane H., Shirai T., Morito H., Yamada T., Hasegawa Y., Ikeda T. (2011): Fabrication of porous SiC ceramics having pores shaped with Si grain templates. Journal of the European Ceramic Society, 31(3), 409-413. Doi: 10.1016/j.jeurceramsoc.2010.10.025
7. Khosravanihaghighi A., Pakshi M. (2017): Effects of SiC particle size on electrochemical and mechanical behavior of SiC-based refractory coatings. Journal of the Australian Ceramic Society, 53(2), 1-7. Doi: 10.1007/s41779-017-0105-z
8. Han L., Huang L., Li F.L., Wang J.K., Pei Y.T., Zeng Y., Jia Q.L., Zhang H.J., Zhang S.W. (2018): Low-temperature preparation of Si_3N_4/SiC porous ceramics via foam-gel-casting and microwave-assisted catalytic nitridation. Ceramics International, 44(10), 11088-11093. Doi: 10.1016/j.ceramint.2018.03.096
9. Ren X.M., Ma B.Y., Su C., Qian F., Yang W.G., Yuan L., Yu J.K., Liu G.Q., Li H.X. (2019): In-situ synthesis of Fe_xSi_y phases and their effects on the properties of SiC porous ceramics. Journal of Alloys and Compounds, 784, 1113-1122. Doi: 10.1016/j.jallcom.2019.01.031

10. You Q.W., Liu Y.S., Wan J.J., Shen Z.J., Li H.X., Yuan B., Cheng L.F., Wang G. (2017): Microstructure and properties of porous SiC ceramics by LPCVI technique regulation. Ceramics International, 43(15), 11855-11863. Doi: 10.1016/j.ceramint.2017.06.031
11. Monteiro R.R., Sabioni A.C.S. (2016): Preparation of mullite whiskers derived from topaz doped with rare earth oxides for applications in composite materials. Ceramics International, 42(1), 49-55. Doi: 10.1016/j.ceramint.2015.08.147
12. Silvestroni L., Sciti D., Melandri C., Guicciarsi S. (2010): Toughened ZrB-based ceramics through SiC whisker or SiC chopped fiber additions. Journal of the European Ceramic Society, 30(11), :2155-2164. Doi: 10.1016/j.jeurceramsoc.2009.11.012
13. Yuan L., Ma B.Y., Zhu Q., Zhang X.D., Zhang H., Yu J.K. (2017): Preparation and properties of mullite-bonded porous fibrous mullite ceramics by an epoxy resin gel-casting process. Ceramics International, 43(7), 5478-5483. Doi: 10.1016/j.ceramint.2017.01.062
14. Yin Y., Ma B.Y., Li S.M., Zhang B.W., Yu J.K., Zhang Z, Li G.Q. (2016): Synthesis of Al_2O_3–SiC composite powders from coal ash in NaCl-KCl molten salts medium. Ceramics International, 42(16), 19225-19230. Doi: 10.1016/j.ceramint.2016.09.087
15. Ren X.M., Ma B.Y., Zhang Y.R., Zhu Q., Li D.X., Li S.M., Yuan L., Yu J.K., Liu G.Q., Li H.X. (2018): Effects of sintering temperature and V_2O_5 additive on the properties of SiC–Al_2O_3 ceramic foams. Journal of Alloys and Compounds, 732, 716-724. Doi: 10.1016/j.jallcom.2017.10.170
16. Wang Y.Q., Tao J., Zhang J.L., Wang T. (2011): Effects of addition of NH_4HCO_3 on pore characteristics and compressive properties of porous Ti-10%Mg composites. Transactions of Nonferrous Metals Society of China, 21(5), 1074-1079. Doi: 10.1016/S1003-6326(11)60824-8
17. Wu J.F., Zhang Y.X., Xu X.H., Deng T.F., Lao X.B., Li K., Xu X.Y. (2016): Thermal shock resistance and oxidation behavior of in-situ synthesized $MgAl_2O_4$–Si_3N_4 composites used for solar heat absorber. Ceramics International, 42 (8), 10175-10183. Doi: 10.1016/j.ceramint.2016.03.133
18. Luo M., Li Y.W., Sang S.B., Zhao L., Jin S.L., Li Y.B. (2012): In situ formation of carbon nanotubes and ceramic whiskers in Al_2O_3–C refractories with addition of Ni-catalyzed phenolic resin. Materials Science and Engineering: A, 558, 533-542. Doi: 10.1016/j.msea.2012.08.044
19. Cetinkaya S., Eroglu S. (2011): Chemical vapor deposition of C on SiO_2 and subsequent carbothermal reduction for the synthesis of nanocrystalline SiC particles/whiskers. International Journal of Refractory Metals and Hard Materials, 29(5), 566-572. Doi: 10.1016/j.ijrmhm.2011.03.005
20. Narciso-Romero F.J., Rodríguez-Reinoso F. (1996): Synthesis of SiC from rice husks catalysed by iron, cobalt or nickel. Journal of Materials Science, 31(3), 779-784. Doi: 10.1007/BF00367899
21. Luo Y., Zheng S.L., Ma S.H., Liu C.L., Wang X.H. (2018): Mullite-bonded SiC-whisker-reinforced SiC matrix composites: Preparation, characterization, and toughening mechanisms. Journal of the European Ceramic Society, 38(16), 5282-5293. Doi: 10.1016/j.jeurceramsoc.2018.08.022